ORIGINAL ARTICLE

WILEY | Journal of Pineal Research
Molecular, Biological, Physiological and
Clinical Aspects of Melatonin

Pan-cancer genomic analyses reveal prognostic and immunogenic features of the tumor melatonergic microenvironment across 14 solid cancer types

Jia-Wei Lv[1] | Zi-Qi Zheng[1] | Zi-Xian Wang[2] | Guan-Qun Zhou[1] | Lei Chen[1,3] | Yan-Ping Mao[1,4] | Ai-Hua Lin[5] | Russel J. Reiter[6] | Jun Ma[1] | Yu-Pei Chen[1] | Ying Sun[1] (iD)

[1]Department of Radiation Oncology, State Key Laboratory of Oncology in South China, Collaborative Innovation Center for Cancer Medicine, Guangdong Key Laboratory of Nasopharyngeal Carcinoma Diagnosis and Therapy, Sun Yat-sen University Cancer Center, Guangzhou, China

[2]Department of Medical Oncology, State Key Laboratory of Oncology in South China, Collaborative Innovation Center for Cancer Medicine, Guangdong Key Laboratory of Nasopharyngeal Carcinoma Diagnosis and Therapy, Sun Yat-sen University Cancer Center, Guangzhou, China

[3]Department of Radiation Oncology, University of Texas MD Anderson Cancer Center, Houston, Texas

[4]Department of Radiation Oncology, University of Michigan, Ann Arbor, Michigan

[5]Department of Medical Statistics and Epidemiology, School of Public Health, Sun Yat-sen University, Guangzhou, China

[6]Department of Cellular and Structure Biology, UT Health, San Antonio, Texas

Correspondence
Ying Sun and Yu-Pei Chen, Department of Radiation Oncology, State Key Laboratory of Oncology in South China, Collaborative Innovation Center for Cancer Medicine, Guangdong Key Laboratory of Nasopharyngeal Carcinoma Diagnosis and Therapy, Sun Yat-sen University Cancer Center, Guangzhou, China.
Emails: sunying@sysucc.org.cn (YS); chenyup1@sysucc.org.cn (YPC)

Abstract

We performed comprehensive genomic analyses of the melatonergic system within the tumor microenvironment and their clinical relevance across a broad spectrum of solid tumors. RNA-seq data from The Cancer Genome Atlas (TCGA) of 14 solid tumors representing 6658 human samples were analyzed. The tumor melatonergic system was characterized by the rates of melatonin synthesis and metabolism using a two-gene expression model (melatonin synthesis/metabolism Index). We calculated three indexes according to different melatonin metabolism isoenzymes (Index-I [*ASMT:CYP1A1*], Index-II [*ASMT:CYP1A2*], and Index-III [*ASMT:CYP1B1*]). Samples of each cancer type were classified into two subgroups (high vs low) based on median values. Clinical outcomes, mutational burden, and neoepitope abundance were analyzed and compared. We found that the ability of the tumor microenvironment to synthesize and accumulate melatonin varied across cancer types and negatively correlated with tumor burden. Kaplan-Meier survival analyses and multivariable modeling showed that the three indexes played different roles across different cancers and harbored prognostic values in breast cancer (adjusted hazard ratio [AHR]$_{\text{Index-II}}$ = 0.65 [0.44-0.97]; P = 0.03), cervical cancer (AHR$_{\text{Index-I}}$ = 0.62 [0.39-0.98]; P = 0.04), lung squamous cell carcinoma (AHR$_{\text{Index-III}}$ = 0.75 [0.56-0.99]; P = 0.04), melanoma (AHR$_{\text{Index-I}}$ = 0.74 [0.55-0.98]; P = 0.04), and stomach adenocarcinoma (AHR$_{\text{Index-III}}$ = 0.68 [0.41-0.94]; P = 0.02). We further investigated its clinical relevance with tumor immunogenic features (mutational burden and neoantigen

Lv, Zheng, Wang, and Zhou contributed equally to this work.

abundance), which may predict immunotherapy benefits. We observed significant negative correlations with mutational burden in the majority of tumors ($P < 0.05$), except cervical cancer, pancreatic adenocarcinoma, and thyroid carcinoma. Our study provides a systematic overview of the oncostatic values of the melatonergic system and highlights the utilization of this simple and promising gene signature as a prognosticator and potential predictor of response to immunotherapy.

KEYWORDS

melatonergic system, molecular marker, mutational burden, neoantigen abundance, pan-cancer analyses, prognosis, tumor microenvironment

1 | INTRODUCTION

Melatonin is a functionally pleiotropic molecular that is secreted primarily by the pineal gland in response to darkness. It provides time-of-day information to the organism and ensures the synchronization of circadian and seasonal rhythms.[1] The natural synthesis of this agent involves a variety of processes.[2] Acetylserotonin O-methyltransferase (ASMT) is the final enzyme of the biosynthetic pathway and has been reported to play a rate-limiting role in melatonin synthesis.[3] In human, melatonin is metabolized by the hepatic cytochromes (primarily CYP1A1, CYP1A2) into 6-hydroxymelatonin (6OH-MEL).[4] Another major metabolic enzyme is CYP1B1, which has a ubiquitous extrahepatic distribution, and has been shown to be expressed at high levels in tissues such as intestine and cerebral cortex.[4] The biosynthetic and metabolic processes influence the level of circulating melatonin. It is well recognized that circulating melatonin exerts a broad range of oncostatic effects through both receptor-dependent and receptor-independent pathways.[5] The interaction of tumor cells, circulating melatonin, and the associated receptors, as well as the surrounding blood vessels, fibroblasts, immune cells, extracellular matrix, and signaling molecules, constitutes the tumor melatonergic microenvironment.[5-7]

The complex interplay between solid tumors and host melatonergic microenvironment has been studied in several cancers. For example, melatonin contributes to the cross talk between cell-cell and cell-matrix adhesion by reducing the expression of $\alpha_v\beta_3$ integrin, which limits glioma cell migration into surrounding stroma.[8] Additionally, melatonin participates in the reduction of surrounding fibroblasts and endothelial cells by downregulating antiadipogenic cytokine expression in breast cancer.[9] However, the majority of these studies were performed on tumor cells or animal models; little has been done to observe the effects of the melatonergic system in patients with malignant diseases. The resulting lack of data has hampered translational research on the antitumor properties of melatonin and further investigation of its therapeutic potentials. The wide impact and clinical relevance of the tumor melatonergic microenvironment make it critical to develop a more thorough understanding of this domain.

Recent years have witnessed the advent of next-generation sequencing (NGS) and large-scale genomics, which has enabled oncological research to move beyond single gene analysis to the integrated investigation of large-volume sequencing data.[10] For example, through The Cancer Genome Atlas (TCGA) project,[11] genomic data of a wide spectrum of cancer types have become available, which greatly deepened our understanding of the genomic features of human cancer. While the tumor melatonin synthesis/metabolism system is thought to differ across varied cancer types, comprehensive genomic analysis of the tumor melatonergic microenvironment (eg, gene expression of melatonin biosynthesis and metabolism, antitumor effects of melatonin, and their interactions with the immune system) has not been adequately explored.

Based on the above data, we conducted a pan-cancer genomic analysis of the tumor melatonergic microenvironment across a broad spectrum of solid tumors, using large-scale RNA-sequencing (RNA-seq) data of TCGA tumor samples. The melatonergic microenvironment is defined by the ratio of two-gene expression (biosynthesis gene expression [*ASMT*] divided by gene expression of the melatonin metabolic enzymes [*CYP1A1/CYP1A2/CYP1B1*]). This is a simple and accessible predictive model to characterize the ability of the tumor microenvironment to synthesize and metabolize melatonin, according to a previously reported study.[12] The aims of this study were to (a) characterize the tumor melatonergic microenvironment across different cancer types; (b) assess the prognostic values of melatonin synthesis/metabolism indexes across varied tumors; and (c) evaluate the associations between melatonin synthesis/metabolism subgroups and immunogenic features (eg, mutational burden and neoantigen abundance), which have been identified as valid biomarkers for predicting response to immune checkpoint inhibitor treatment.[13,14]

2 | MATERIALS AND METHODS

2.1 | Dataset and tumor types

The dataset used consisted of RNA-seq data from TCGA tumor samples (data accessed at cBioPortal for Cancer Genomics in June 2018, http://www.cbioportal.org/).[15,16] All samples were assayed by RNA-seq, as described by the TCGA Research Network.[17] Gene expression values were represented as RNA-Seq by Expectation Maximization (RSEM) data normalized within each sample to the upper quartile of total reads.[18] The degree of mutational burden and presence of neoantigen were adopted to assess the immunogenic features of the tumors.[13,14] The mutational burden was calculated according to the method described by Ock et al[19]; the mutational burden was measured by the total number of somatic mutations, including nonsynonymous mutations, insertion-deletion mutations, and silent mutations, while germline mutations without somatic mutations were excluded. Neoantigen abundance was calculated according to a previous study by Rooney et al[20]; if the mutation was predicted to produce a "binder" neopeptide with affinity <500 nM, and if the corresponding gene was expressed >10 TPM (evaluated based on median expression in the given tumor type rather than the specific sample), the mutation was designated as putatively antigenic. In this study, data of mutational burden and neoantigen abundance were referenced from these two studies; detailed methods are described in published works.[19,20] Colon and rectal adenocarcinoma and pancreatic adenocarcinoma were excluded from analyses as the neoantigen number was only available for three samples. Clinical and pathological information were obtained from the cBioPortal for Cancer Genomics.

Collectively, samples of 14 solid cancer types (N = 6658) were investigated in the final analysis, including bladder urothelial carcinoma (BLCA, n = 406), breast cancer (BRCA, n = 1098), cervical cancer (CESC, n = 306), colon and rectal adenocarcinoma (COAD, n = 376), head and neck squamous cell carcinoma (HNSC, n = 520), kidney clear cell carcinoma (KIRC, n = 534), liver hepatocellular carcinoma (LIHC, n = 359), lung adenocarcinoma (LUAD, n = 508), lung squamous cell carcinoma (LUSC, n = 495), pancreatic adenocarcinoma (PAAD, n = 179), prostate adenocarcinoma (PRAD, n = 498), skin cutaneous melanoma (SKCM, n = 463), stomach adenocarcinoma (STAD, n = 407), and thyroid carcinoma (THCA, n = 509).

2.2 | Predictive model of the melatonergic microenvironment

Gene expression of *ASMT, CYP1A1, CYP1A2*, and *CYP1B1* was measured using log 2-transformed values in RSEM. As per the study of Kinker et al,[12] the tumor melatonergic microenvironment was measured by the rates of melatonin synthesis and metabolism. To characterize the melatonergic microenvironment across different tumor types in more detail, we calculated the following three indexes according to different melatonin metabolism isoenzymes: Index-I $(ASMT:CYP1A1) = \log_2 [ASMT] - \log_2 [CYP1A1]$; Index-II $(ASMT:CYP1A2) = \log_2 [ASMT] - \log_2 [CYP1A2]$; Index-III $(ASMT:CYP1B1) = \log_2 [ASMT] - \log_2 [CYP1B1]$. The gene expressions of CYP1A1/CYP1A2/CYP1B1 were chosen here as they have been shown to play major roles in melatonin metabolism in humans according to published evidence.[4] To further explore the relationships between melatonergic microenvironment, patient prognosis, mutational burden, and neoantigen abundance, we classified the melatonergic system into high versus low subgroups by the median value for each cancer type.

2.3 | Gene set enrichment analysis

To understand the differences in biological functions and pathways between subgroups, gene set enrichment analysis (GSEA, http://software.broadinstitute.org/gsea/index.jsp, accessed at June, 2018) was performed on low- versus high-Index subgroups.[21] We employed the Molecular Signatures Database (MSigDB) H (hallmark gene sets), C2 (curated gene sets), and C5 (GO gene sets) collection of chemical and genetic perturbations (n = 20 253 gene sets). Calculations were repeated 1000 times for each analysis according to the default weighted enrichment statistical method. GSEA results were shown using normalized enrichment scores, accounting for the size and degree to which a gene set is overrepresented at the top or bottom of the ranked list of genes (nominal *P*-value <0.05 and FDR ≤0.25).

2.4 | Statistical analyses

Associations between melatonin synthesis/metabolism subgroups and categorical variables (eg, sex, race, and disease stage) were analyzed using the chi-square test (Fisher's exact test or Pearson's chi-square test where appropriate), and the Mann-Whitney *U* test or Kruskal-Wallis test for continuous variables (eg, age, number of mutations, and neoantigens). Correlations between gene expression were evaluated using the Spearman correlation test; the Spearman coefficient was considered to indicate poor correlation if <0.2, moderate if <0.4, relatively strong if <0.6, strong if <0.8, and very strong if >0.8. The prognostic significance of the indexes was estimated using Kaplan-Meier survival curves and compared by log-rank test. Cox proportional hazards model was used to calculate the adjusted hazard ratios (AHRs) and corresponding 95% confidence intervals (CIs), incorporating age, sex, race, and disease stage for adjustment. All statistical analyses were performed with SPSS version 23.0 (SPSS Inc, Chicago, IL, USA) and R version 3.4.4 (http://www.r-project.org). Statistical significance was set at two-sided *P* < 0.05.

4 of 13 | WILEY— Journal of **Pineal Research**
Molecular, Biological, Physiological and Clinical Aspects of Melatonin

LV ET AL.

3 | RESULTS

3.1 | Characteristics of the melatonergic microenvironment across 14 cancer types

A total of 6658 tumor samples from 14 TCGA cancer types were included in the final analysis. The baseline characteristics are summarized in Table S1. Figure 1 showed the log$_2$-transformed values of *ASMT/CYP1A1/CYP1A2/CYP1B1* expression according to cancer types. The expression of *CYP1A1* and *CYP1A2* was significantly and positively correlated ($R^2_{overall} = 0.62$; Pearson correlation), with moderate to strong correlations for each cancer type (Figure S1), while the expression of *CYP1B1* and *CYP1A1/CYP1A2* did not show strong correlations ($R^2 < 0.40$ for all; Pearson correlation).

Given that the gene expression of metabolism isoenzymes was different in each cancer type, we comprehensively calculated three synthesis/metabolism indexes (Index-I [*ASMT:CYP1A1*], Index-II [*ASMT:CYP1A2*], and Index-III [*ASMT:CYP1B1*]; Figure 1). Overall, the median value of Index-I, Index-II, and Index-III was −0.36 (interquartile range [IQR], −1.99 to 0.50), 0.00 (IQR, −0.49 to 0.93), and −8.32 (IQR, −9.78 to −6.55), respectively. Each cancer type demonstrated heterogeneous distributions of the three indexes. We then divided the samples into two subgroups (high vs low) by the median values of each cancer type. The demographic and clinical features of the TCGA patients were summarized according to synthesis/metabolism subgroups in Table S2. Consistent with previous observations,[12,22,23] elderly patients tended to have lower melatonin synthesis/metabolism Index, with significant differences observed in BRCA, LIHC, LUAD, LUSC, PRAD, and SKCM; the high-Index subgroup also tended to have a lower proportion of patients with late-stage disease, with significant differences observed in CESC, COAD, HNCS, KIRC, SKCM, and THCA.
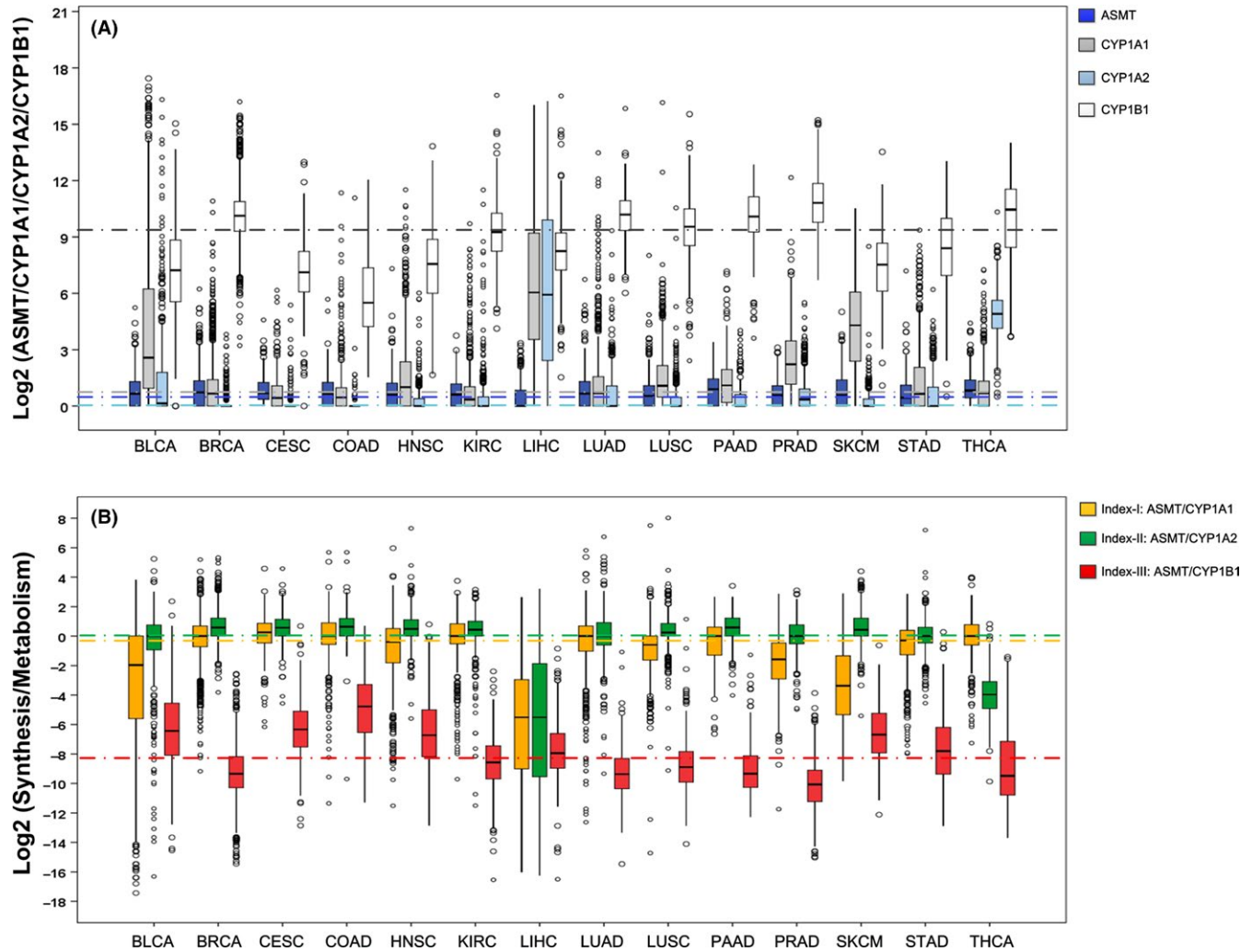
FIGURE 1 Distributions of gene expression of *ASMT, CYP1A1, CYP1A2, CYP1B1*, and melatonin synthesis/metabolism Index-I/II/III across 14 TCGA solid tumors. A, Boxplot distributions of log$_2$-transformed values of *ASMT, CYP1A1, CYP1A2*, and *CYP1B1* according to TCGA cancer types. B, Boxplot distributions of log$_2$-transformed values of melatonin synthesis/metabolism Index (Index-I [*ASMT:CYP1A1*], Index-II [*ASMT:CYP1A2*], and Index-III [*ASMT:CYP1B1*]), according to TCGA cancer types. The dashed lines indicate the median values of all tumor samples

3.2 | Favorable prognoses were correlated with the high melatonin synthesis/metabolism Index subgroup

We investigated the prognostic association of the tumor melatonergic microenvironment with clinical outcomes. As the distributions of the three indexes differed significantly among 14 cancer types, we then evaluated whether they played different prognostic roles across varied cancers. Figure 2 summarized the results of Kaplan-Meier survival analyses. On the whole, almost all patients in the high synthesis/metabolism Index subgroup had relatively favorable clinical outcomes, compared to patients in the low-Index subgroup; while for each cancer type, the three indexes harbored different prognostic values. Specifically, for Index-I, the high-Index subgroup showed significantly improved survival among patients with CESC ($P = 0.01$) and PAAD ($P = 0.04$), while marginal significance among patients with SKCM ($P = 0.09$) and STAD ($P = 0.08$) was also observed. In terms of Index-II, only patients with BRCA and STAD showed marginally significantly ($P \leq 0.10$) improved survival in the high-Index subgroups. Regarding Index-III, BLCA ($P = 0.02$), COAD ($P = 0.03$), KIRC ($P = 0.03$), and STAD ($P = 0.03$) showed favorable prognosis among patients with a high synthesis/metabolism Index.

Next, we performed multivariable analysis to explore whether melatonin synthesis/metabolism Index was an independent prognostic factor for survival outcomes, incorporating clinically relevant covariates for adjustment. The results of multivariable modeling largely supported the findings seen in the univariate analysis. Interestingly, the three indexes all remained significant prognostic factors for STAD ($AHR_{Index-I} = 0.71$; 95% CI = 0.52-0.97, $P = 0.03$; $AHR_{Index-II} = 0.69$; 95% CI = 0.49-0.97, $P = 0.03$; $AHR_{Index-III} = 0.68$; 95% CI = 0.41-0.94; $P = 0.02$; Figure 3). Index-I was an independent and favorable prognosticator for patients with CESC ($AHR = 0.62$; 95% CI = 0.39-0.98; $P = 0.04$) and SKCM ($AHR = 0.74$; 95% CI = 0.55-0.98; $P = 0.04$). The high-Index-II subgroup had significantly better survival among patients with BRCA ($AHR = 0.65$; 95% CI = 0.44-0.97; $P = 0.03$), and Index-III remained significant for LUSC ($AHR = 0.75$; 95% CI = 0.56-0.99; $P = 0.04$). PRAD and THCA were excluded from multivariable analyses due to the limited number of events. Cox proportional hazards analyses of other clinical-relevant covariates for adjustment were shown in Table S3.

3.3 | High mutational burden was associated with the low melatonin synthesis/metabolism Index subgroup

Previous studies have reported a physiological link between the pineal gland and immune system.[24,25] Additionally, emerging evidence has shown that the degree of mutational burden and presence of neoantigen reflect tumor immunogenic features, and can predict favorable responses to immune blockade therapy (eg, anti-PD-1/PD-L1 treatment).[13,14] We therefore further compared melatonin synthesis/metabolism subgroups according to the mutational burden and neoantigen abundance. We observed a tendency toward a negative correlation between the total number of somatic mutations (Figure 4), as well as the number of neoantigens (Figure 5) with the synthesis/metabolism Index. Based on cancer types, the low-Index subgroup had both a significantly higher number of mutations and neoantigens among patients with HNSC (Index-I), KIRC (Index-I), PRAD (Index-I and Index-II), and STAD (Index-III), compared to patients with a high synthesis/metabolism Index ($P < 0.05$ for all). Additionally, patients with BRCA (Index-II), COAD (Index-I), KIRC (Index-I), LIHC (Index-I), LUSC (Index-III), PAAD (Index-III), and SKCM (Index-I) had a significantly higher number of somatic mutations in the low-Index subgroup ($P < 0.05$ for all, Figure 4B,D,F,G,I). BLCA (Index-II) and KIRC (Index-III) tumors with low melatonin synthesis/metabolism Index harbored a higher number of neoantigens ($P < 0.05$ for all, Figure 5A,E). No significant differences were observed regarding the numbers of mutations or neoantigens for CESC or THCA.

3.4 | Gene set enrichment analyses of melatonin synthesis/metabolism subgroups

We then performed GSEA to better understand how the melatonergic microenvironment functioned through potential biological pathways. We chose BRCA (Index-II), LUSC (Index-III), SKCM (Index-I), and STAD (Index-III) as study models, as the melatonergic microenvironment influenced both prognosis and immunogenic features in these four tumors. Figure S2 and Table S4-S7 illustrated the gene sets enriched in high and low melatonin synthesis/metabolism subgroups. Generally, gene sets related to hypoxia, inflammation, proliferation, metastasis, and DNA damage were enriched in the low-Index subgroup, indicating that melatonin may play an antitumor role in cancer development and progression.

3.5 | Summary of the clinical implications of melatonergic microenvironment classification

Figure 6 summarized the biological and clinical relevance of tumor melatonergic microenvironment classification. Taken together, our data demonstrated that among patients with BRCA, LUSC, SKCM, and STAD, decreased melatonin synthesis/metabolism indexes, which characterized the rates of circulating melatonin synthesis and metabolism in tumor

6 of 13 | WILEY — *Journal of* **Pineal Research** — Molecular, Biological, Physiological and Clinical Aspects of Melatonin
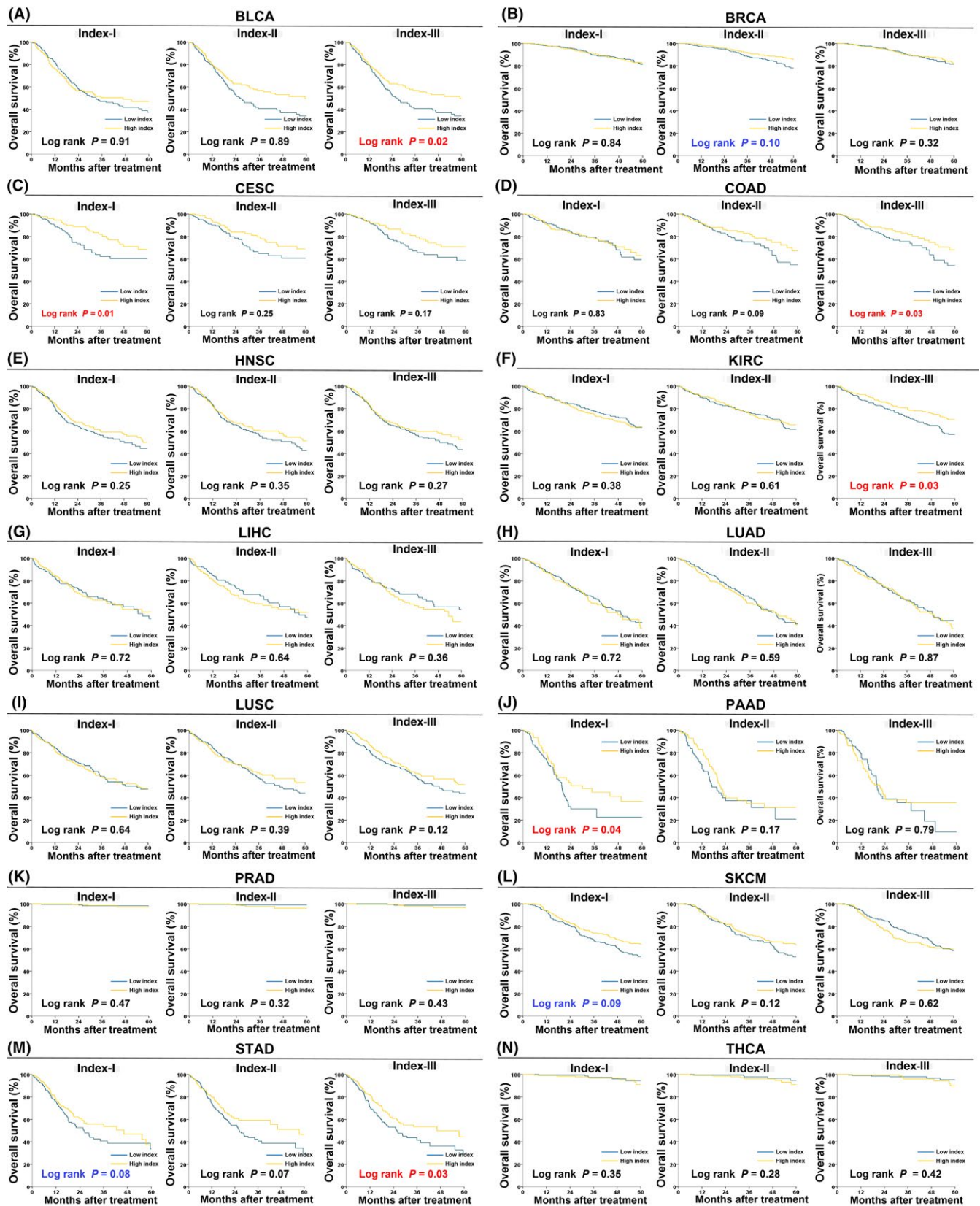
LV ET AL.

FIGURE 2 Kaplan-Meier plots of overall survival for patients in different melatonin synthesis/metabolism subgroups across 14 TCGA solid tumors. (A) BLCA, (B) BRCA, (C) CESC, (D) COAD, (E) HNSC, (F) KIRC, (G) LIHC, (H) LUAD, (I) LUSC, (J) PRAD, (K) PRAD, (L) SKCM, (M) STAD, (N) THCA $P < 0.05$ represents significant differences in survival outcomes
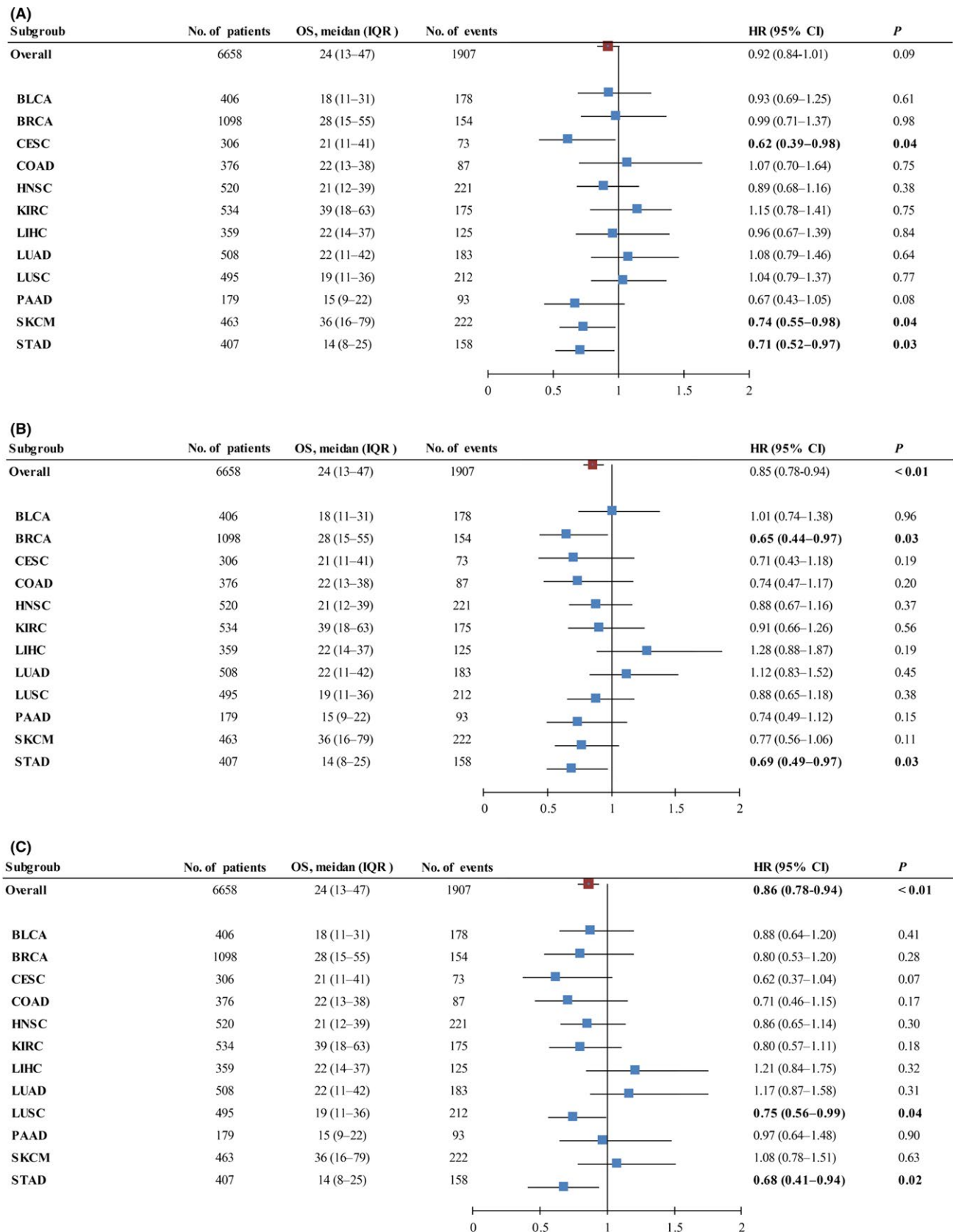
(A)

Subgroub	No. of patients	OS, meidan (IQR)	No. of events	HR (95% CI)	P
Overall	6658	24 (13–47)	1907	0.92 (0.84–1.01)	0.09
BLCA	406	18 (11–31)	178	0.93 (0.69–1.25)	0.61
BRCA	1098	28 (15–55)	154	0.99 (0.71–1.37)	0.98
CESC	306	21 (11–41)	73	**0.62 (0.39–0.98)**	**0.04**
COAD	376	22 (13–38)	87	1.07 (0.70–1.64)	0.75
HNSC	520	21 (12–39)	221	0.89 (0.68–1.16)	0.38
KIRC	534	39 (18–63)	175	1.15 (0.78–1.41)	0.75
LIHC	359	22 (14–37)	125	0.96 (0.67–1.39)	0.84
LUAD	508	22 (11–42)	183	1.08 (0.79–1.46)	0.64
LUSC	495	19 (11–36)	212	1.04 (0.79–1.37)	0.77
PAAD	179	15 (9–22)	93	0.67 (0.43–1.05)	0.08
SKCM	463	36 (16–79)	222	**0.74 (0.55–0.98)**	**0.04**
STAD	407	14 (8–25)	158	**0.71 (0.52–0.97)**	**0.03**

(B)

Subgroub	No. of patients	OS, meidan (IQR)	No. of events	HR (95% CI)	P
Overall	6658	24 (13–47)	1907	0.85 (0.78–0.94)	**< 0.01**
BLCA	406	18 (11–31)	178	1.01 (0.74–1.38)	0.96
BRCA	1098	28 (15–55)	154	**0.65 (0.44–0.97)**	**0.03**
CESC	306	21 (11–41)	73	0.71 (0.43–1.18)	0.19
COAD	376	22 (13–38)	87	0.74 (0.47–1.17)	0.20
HNSC	520	21 (12–39)	221	0.88 (0.67–1.16)	0.37
KIRC	534	39 (18–63)	175	0.91 (0.66–1.26)	0.56
LIHC	359	22 (14–37)	125	1.28 (0.88–1.87)	0.19
LUAD	508	22 (11–42)	183	1.12 (0.83–1.52)	0.45
LUSC	495	19 (11–36)	212	0.88 (0.65–1.18)	0.38
PAAD	179	15 (9–22)	93	0.74 (0.49–1.12)	0.15
SKCM	463	36 (16–79)	222	0.77 (0.56–1.06)	0.11
STAD	407	14 (8–25)	158	**0.69 (0.49–0.97)**	**0.03**

(C)

Subgroub	No. of patients	OS, meidan (IQR)	No. of events	HR (95% CI)	P
Overall	6658	24 (13–47)	1907	**0.86 (0.78–0.94)**	**< 0.01**
BLCA	406	18 (11–31)	178	0.88 (0.64–1.20)	0.41
BRCA	1098	28 (15–55)	154	0.80 (0.53–1.20)	0.28
CESC	306	21 (11–41)	73	0.62 (0.37–1.04)	0.07
COAD	376	22 (13–38)	87	0.71 (0.46–1.15)	0.17
HNSC	520	21 (12–39)	221	0.86 (0.65–1.14)	0.30
KIRC	534	39 (18–63)	175	0.80 (0.57–1.11)	0.18
LIHC	359	22 (14–37)	125	1.21 (0.84–1.75)	0.32
LUAD	508	22 (11–42)	183	1.17 (0.87–1.58)	0.31
LUSC	495	19 (11–36)	212	**0.75 (0.56–0.99)**	**0.04**
PAAD	179	15 (9–22)	93	0.97 (0.64–1.48)	0.90
SKCM	463	36 (16–79)	222	1.08 (0.78–1.51)	0.63
STAD	407	14 (8–25)	158	**0.68 (0.41–0.94)**	**0.02**

FIGURE 3 Cox proportional hazards analyses of melatonin synthesis/metabolism (A) Index-I, (B) Index-II, and (C) Index-III across 14 TCGA solid tumors. Note: age (continuous variable), sex (Male vs Female), race (White vs Asian vs Black vs American Indian vs Others), and disease stage (stage III-IV vs stage I-II) were included in the multivariable model for adjustment. PRAD and THCA were excluded from the analyses due to the limited number of events
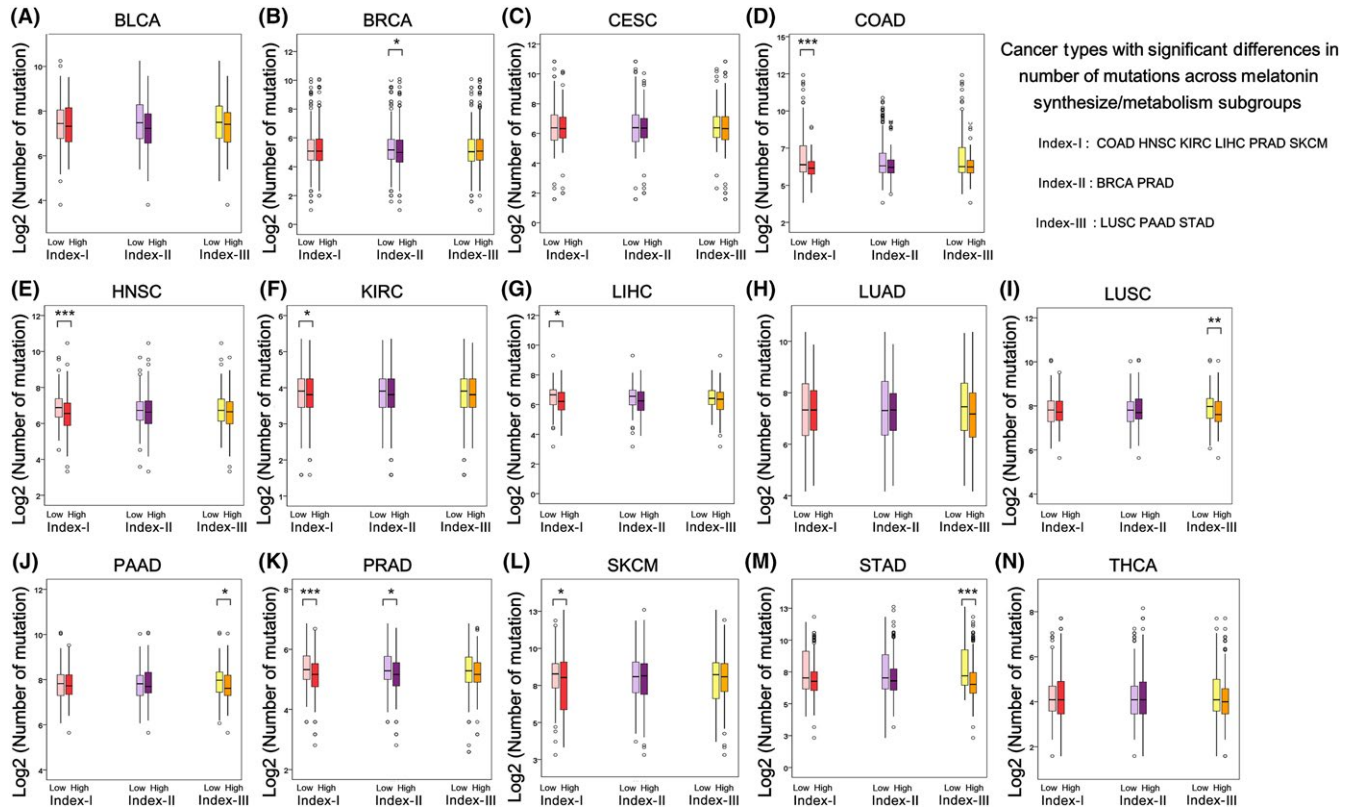
FIGURE 4 Mutational burdens by different melatonin synthesis/metabolism subgroups across TCGA solid tumors. Boxplot distributions of $\log_2$-transformed values of the number of somatic mutations between subgroups of melatonin synthesis/metabolism indexes I-III, according to TCGA cancer types (A-N). The number of mutations differed significantly in Index-I subgroups for COAD, HNSC, KIRC, LIHC, PRAD, and SKCM; in Index-II subgroups for BRCA and PRAD; and in Index-III subgroups for LUSC, PAAD, and STAD *P* values are calculated by Wilcoxon rank-sum test (*$P < 0.05$, **$P < 0.01$, ***$P < 0.001$)

microenvironment, were associated with reduced survival, as well as higher levels of somatic mutations and neoantigens, which indicated favorable responses to immunotherapy. For CESC tumors, melatonergic microenvironment is only correlated with prognosis, while in HNSC, KIRC, and PRAD, patients with decreased melatonin are more likely to benefit from immune checkpoint inhibitor treatment.

4 | DISCUSSION

Here, we present several key aspects of the tumor melatonergic microenvironment based on *ASMT* and *CYP1A1/1A2/1B1* mRNA expression, determined from RNA-seq data across large-scale TCGA solid tumor samples. Initially, we applied a two-gene expression signature (melatonin synthesis/metabolism Index) to characterize the melatonergic system across 14 solid tumors. Having noted that gene expression of melatonin metabolism isoenzymes differed in each cancer type, we further used three indexes (Index-I [*ASMT:CYP1A1*], Index-II [*ASMT:CYP1A2*], and Index-III [ASMT:CYP1B1]) to comprehensively analyze the melatonergic system and compare their roles. We found that the

ability of the tumor microenvironment to synthesize and accumulate melatonin was heterogeneous and negatively correlates with tumor burden, while this ability deceased with age. Secondly, we divided the samples into two subgroups (high vs low) based on the median of Index values and investigated their roles in predicting survival outcomes. We show that the three indexes played different roles across varied cancers, and harbored prognostic value in BRCA, CESC, LUSC, SKCM, and STAD. Next, we determined the clinical relevance of the three indexes with tumor immunogenic features and potential predictive values in selecting patients that may be more responsive to immunotherapies, in light of its negative correlations with mutational burden (number of somatic mutations and/or neoantigens) in BLCA, BRCA, COAD, HNSC, KIRC, LIHC, LUSC, PRCA, SKCM, and STAD. To our knowledge, this is the first comprehensive genomic investigation of the tumor melatonergic microenvironment across a large spectrum of solid tumors, which provides a general overview of the oncostatic value of the melatonergic system.

In this study, a simple and readily adapted gene expression signature was applied to characterize the tumor melatonergic microenvironment. Additionally, we used three
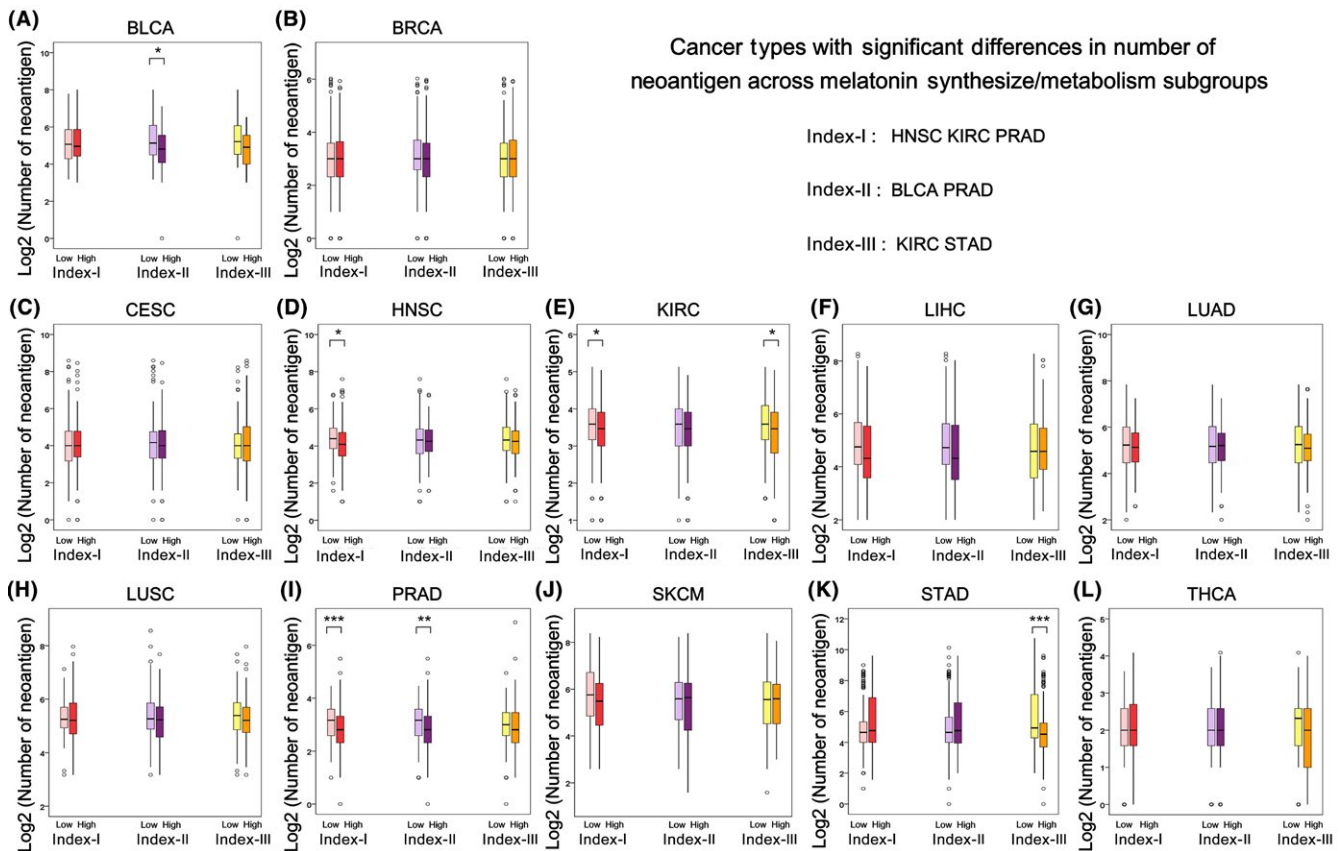
FIGURE 5 Neoantigen abundance by different melatonin synthesis/metabolism subgroups across TCGA solid tumors. Boxplot distributions of $\log_2$-transformed values of the number of neoantigens between subgroups of melatonin synthesis/metabolism indexes I-III, according to TCGA cancer types (A-I). The number of neoantigens differed significantly in Index-I subgroups for HNSC, KIRC, and PRAD; in Index-II subgroups for BLCA and PRAD; and in Index-III subgroups for KIRC and STAD *P* values are calculated by Wilcoxon rank-sum test (*$P < 0.05$, **$P < 0.01$, ***$P < 0.001$). COAD and PAAD are excluded from the analysis due to the limited number of patients with neoantigen data

indexes based on the melatonin metabolism isoenzymes, which provided a comprehensive and applicable model for clinical utilization. We further identified the differential values of the three indexes across varied cancer types, suggesting that the melatonergic synthesis and metabolism system may work through different isoenzymes and pathways in each tumor. Further experimental studies are needed to reveal the underlying mechanisms. The classification of the tumor melatonergic microenvironment according to this model may be a useful tool for risk stratification and will hopefully aid in the design of future experimental and clinical studies. Specifically, we found that higher content of melatonin in the tumor microenvironment was associated with less aggressive stage classification and favorable prognosis, which suggested that the melatonergic microenvironment may influence tumor carcinogenesis, prevent the formation of aggressive phenotypes, and therefore result in a decreased risk of death. This is consistent with previous observations that melatonin reduces the susceptibility of gastric mucosal cells to dietary carcinogens through enhanced DNA repair capacity,[26] and inhibits cancer cell

proliferation by decreasing DNA synthesis[27] or promoting cell differentiation.[28] Additionally, we demonstrated that the melatonin synthesis/metabolism Index remained an independent prognosticator after including disease stage for adjustment in multivariable models, which implied that melatonin may influence prognosis through other biological mechanisms in addition to tumor carcinogenesis and proliferation. For instance, it was noted that melatonin impeded the epithelial-mesenchymal transition (EMT) process and cancer cell dissemination through interference with NF-κB signaling.[29] Melatonin also promotes cancer cell apoptosis by inducing cell cycle arrest.[30] Another phenomenon worth noting is that *CYP1B1* overexpression itself could enhance proliferation, migration, and invasion of tumor cells in prostate cancer and kidney cancer.[31,32] Therefore, inferior survival in the low-Index-III subgroup might also be attributable to overexpression of *CYP1B1* in some cancer types; further experimental studies are needed to reveal the underlying mechanism in different cancer types in this note. The valid associations between melatonin and risk of death have facilitated randomized controlled clinical trials
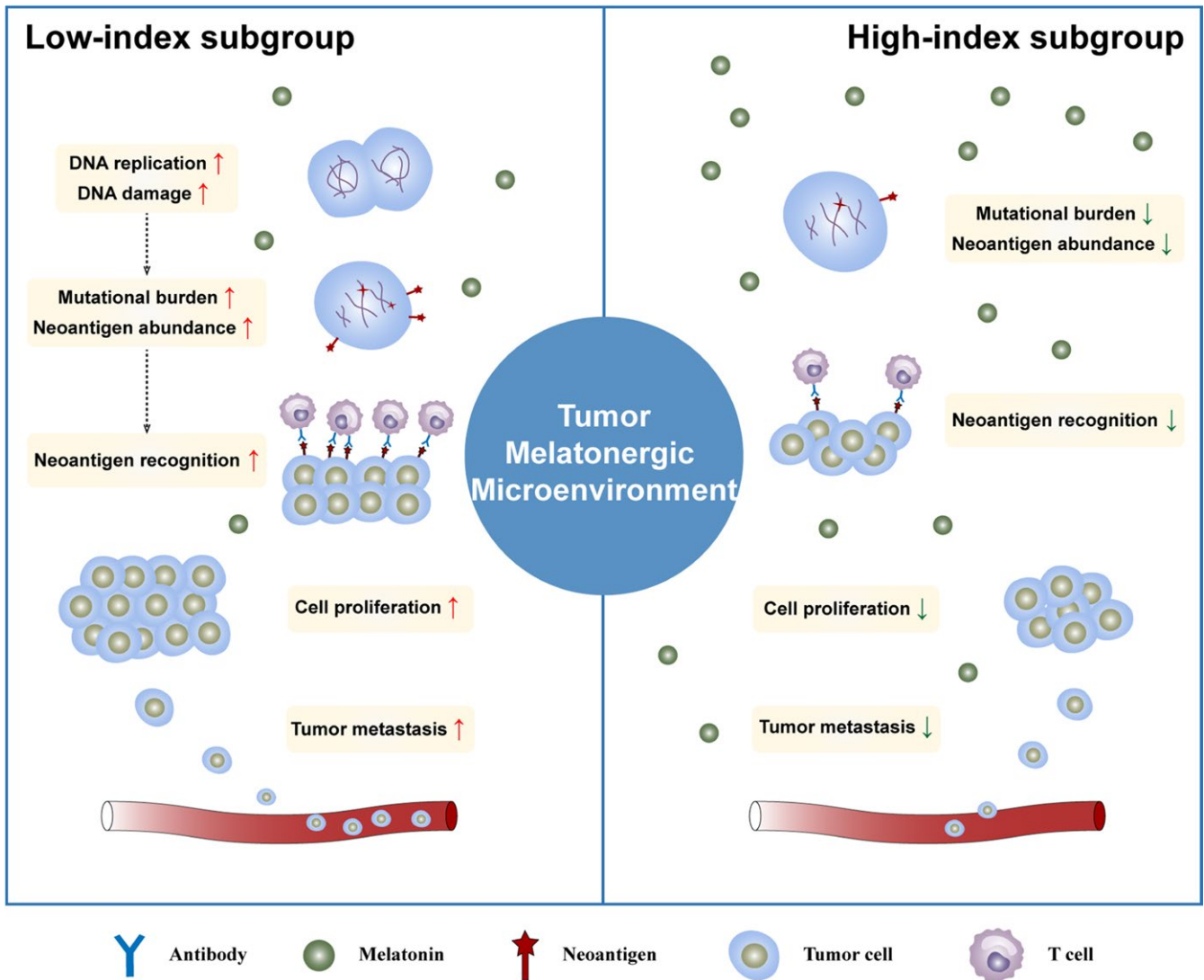
FIGURE 6 Biological and clinical relevance of the tumor melatonergic microenvironment classification based on a two-gene mRNA expression model. The tumor melatonergic microenvironment is categorized into high vs low subgroups based on median values of melatonin synthesis/metabolism Index. The high-Index subgroup is characterized by higher content of circulating melatonin, less aggressive tumor biological behaviors (eg, cell proliferation, metastasis), favorable prognosis, etc, while the low-Index subgroup harbors a higher number of somatic mutations and neoantigens, and would potentially be more likely to respond to immune checkpoint inhibitor treatment. The proposed classification is simple and applicable and would help tailor optimal therapeutic strategies for solid tumors

(RCTs) investigating the therapeutic roles of melatonin in improving survival outcomes and tumor responses. Lissoni et al[33] indicated that melatonin significantly improved tumor regression rate and 5-year overall survival in non–small-cell lung cancer patients concomitantly treated with melatonin and chemotherapy. A meta-analysis systematically analyzed eight published RCTs and showed that melatonin dramatically improved tumor remission and 1-year survival rate, as well as decreased the incidence of treatment-related toxicity.[34] While the above results are inspiring, published RCTs only refer to a limited spectrum of tumors (glioma,[35] COAD,[36] and LUSC[33,37]). Based on our findings, we propose the conduction of more collaborative international, multi-center, large-scale RCTs in a variety

of cancer types, especially in patients with BRCA, CESC, LUSC, SKCM, and STAD.

In addition to its prognostic implication, the tumor melatonergic environment also distinguished patients with distinct immunogenic features. Our findings indicated that patients with a low melatonin synthesis/metabolism Index tended to harbor a higher number of somatic mutations and/or neoantigens, and would be potentially more likely to benefit from immunotherapies. Somatic genome instability is a hallmark of cancer genomes, and a highly complex mutation landscape has been reported to originate from distinct DNA damage and repair processes.[38] Previous research has also demonstrated that somatic mutations can subsequently generate neoantigens,[13,14] which in turn could be recognized

by the immune system, triggering an anticancer immune response and therefore likely to be associated with favorable responses to immunotherapy.[39] In this vein, melatonin in the tumor microenvironment could significantly limit the extent of DNA damage and enhance DNA repair processes,[40] which potentially explained the lower mutational burden and neoantigen abundance in the high-Index subgroup. A considerable number of published studies have explored the immune-neuroendocrine role of melatonin,[41,42] while less work has been done to evaluate its predictive value for the immune response in solid tumors. The analysis of associations between the melatonergic microenvironment and tumor immunogenic features represents a novel aspect of melatonin research and highlights the importance of future investigations on the immunotherapeutic role of melatonin across diverse tumor types.

Among the solid tumors investigated in this study, several cancer types (eg, LUAD, PAAD, and THCA) were found to neither correlate with clinical prognosis nor the number of mutations and neoantigens. The failure to detect associations in TCGA data may be due to lack of adequate follow-up time, limited event rates, and biased population distribution, among other considerations. Additionally, it also suggests that our two-gene predictive model alone is not sufficient to stratify those groups of individuals; integration of other melatonergic molecular biomarkers (eg, expression of melatonin receptors[43]) is needed in future investigations. Nevertheless, although melatonin synthesis/metabolism Index alone could not substitute for traditional parameters to predict survival outcome, it may facilitate the establishment of optimal prediction models when incorporated with other clinicopathological factors. Importantly, this simple model can be readily adapted to PCR-based analysis of formalin-fixed paraffin-embedded (FFPE) clinical specimens, which is extremely efficient and cost-effective.

The main limitation of this study is that the ability of these indexes to predict the response to immunotherapy requires further validation in cancer patients treated with immune checkpoint inhibitors. Future studies are needed to address this limitation. Nevertheless, our findings are important and provide new insights into the melatonergic microenvironment of solid tumors. Secondly, we only adopted the gene expression of three enzymes involved in melatonin metabolism (*CYP1A1, CYP1A2,* and *CYP1B1*) to establish the two-gene indexes. Future studies that comprehensively investigate and compare different metabolic enzymes and their combinations are warranted. Thirdly, the evidence that the two-gene Index could represent circulating melatonin in the tumor microenvironment was derived from previous research in glioma.[12] However, given the distinct contexts of different tumors, future experiments are needed to verify the associations between circulating melatonin and the two-gene indexes across different cancer types.

5 | CONCLUSION

In conclusion, we comprehensively characterized the melatonergic microenvironment across 14 solid tumors using RNA-seq data from TCGA. Our findings revealed that the capacity of the tumor microenvironment to synthesize and accumulate melatonin can distinguish patients with different risks. Additionally, it correlated with tumor immunogenic features (mutational burden and neoantigen abundance) and served as a potential predictive marker in selecting patients responsive to immunotherapies. Our study provides a systematic overview of the oncostatic values of the melatonergic system and highlights the utilization of a simple and promising two-gene signature for clinical practice. Going forward, it lays groundwork for the design of future experimental and clinical studies.

CONFLICT OF INTEREST

The authors have no actual or potential conflicts of interest to declare.

AUTHOR CONTRIBUTIONS

Ying Sun, Yu-Pei Chen, and Jia-Wei Lv involved in conception and design of the study. Ying Sun provided financial support. Ying Sun, Yu-Pei Chen, and Jun Ma provided administrative support. Ying Sun, Yu-Pei Chen, and Jia-Wei Lv carried out provision of study materials or patients. Jia-Wei Lv, Zi-Qi Zheng, Zi-Xian Wang, Guan-Qun Zhou, Lei Chen, and Yan-ping Mao involved in collection and assembly of data. Jia-Wei Lv, Zi-Qi Zheng, Guan-Qun Zhou, Ai-Hua Lin, and Yu-Pei Chen analyzed and interpreted the data. All authors involved in manuscript writing and final approval of the manuscript.

12 of 13 | **WILEY**—Journal of **Pineal Research**
Molecular, Biological, Physiological and
Clinical Aspects of Melatonin

LV ET AL.

ORCID

Ying Sun (iD) https://orcid.org/0000-0002-5888-2929

REFERENCES

1. Vriend J, Reiter RJ. Melatonin feedback on clock genes: a theory involving the proteasome. *J Pineal Res*. 2015;58:1-11.

2. Simonneaux V, Ribelayga C. Generation of the melatonin endocrine message in mammals: a review of the complex regulation of melatonin synthesis by norepinephrine, peptides, and other pineal transmitters. *Pharmacol Rev*. 2003;55:325-395.

3. Botros HG, Legrand P, Pagan C, et al. Crystal structure and functional mapping of human ASMT, the last enzyme of the melatonin synthesis pathway. *J Pineal Res*. 2013;54:46-57.

4. Ma X, Idle JR, Krausz KW, et al. Metabolism of melatonin by human cytochromes p450. *Drug Metab Dispos*. 2005;33:489-494.

5. Su SC, Hsieh MJ, Yang WE, et al. Cancer metastasis: mechanisms of inhibition by melatonin. *J Pineal Res*. 2017;62:e12370.

6. Maschio-Signorini LB, Gelaleti GB, Moschetta MG, et al. Melatonin regulates angiogenic and inflammatory proteins in MDA-MB-231 cell line and in co-culture with cancer-associated fibroblasts. *Anticancer Agents Med Chem*. 2016;16:1474-1484.

7. Jardim-Perassi BV, Lourenco MR, Doho GM, et al. Melatonin regulates angiogenic factors under hypoxia in breast cancer cell lines. *Anticancer Agents Med Chem*. 2016;16:347-358.

8. Xu CS, Wang ZF, Huang XD, et al. Involvement of ROS-alpha v beta 3 integrin-FAK/Pyk2 in the inhibitory effect of melatonin on U251 glioma cell migration and invasion under hypoxia. *J Transl Med*. 2015;13:95.

9. Alvarez-Garcia V, Gonzalez A, Alonso-Gonzalez C, et al. Melatonin interferes in the desmoplastic reaction in breast cancer by regulating cytokine production. *J Pineal Res*. 2012;52:282-290.

10. Marx V. Next-generation sequencing: the genome jigsaw. *Nature*. 2013;501:263-268.

11. The Cancer Genome Atlas Research Network, Weinstein JN, Collisson EA, et al. The Cancer Genome Atlas Pan-Cancer analysis project. *Nat Genet*. 2013;45:1113-1120.

12. Kinker GS, Oba-Shinjo SM, Carvalho-Sousa CE, et al. Melatonergic system-based two-gene index is prognostic in human gliomas. *J Pineal Res*. 2016;60:84-94.

13. Schumacher TN, Schreiber RD. Neoantigens in cancer immunotherapy. *Science*. 2015;348:69-74.

14. Rizvi NA, Hellmann MD, Snyder A, et al. Cancer immunology. Mutational landscape determines sensitivity to PD-1 blockade in non-small cell lung cancer. *Science*. 2015;348:124-128.

15. Cerami E, Gao J, Dogrusoz U, et al. The cBio cancer genomics portal: an open platform for exploring multidimensional cancer genomics data. *Cancer Discov*. 2012;2:401-404.

16. Gao J, Aksoy BA, Dogrusoz U, et al. Integrative analysis of complex cancer genomics and clinical profiles using the cBioPortal. *Sci Signal*. 2013;6:pl1.

17. Cancer Genome Atlas Research Network. Comprehensive genomic characterization of squamous cell lung cancers. *Nature*. 2012;489:519-525.

18. Palmer C, Diehn M, Alizadeh AA, et al. Cell-type specific gene expression profiles of leukocytes in human peripheral blood. *BMC Genom*. 2006;7:115.

19. Ock CY, Keam B, Kim S, et al. Pan-cancer immunogenomic perspective on the tumor microenvironment based on PD-L1 and CD8 T-cell infiltration. *Clin Cancer Res*. 2016;22:2261-2270.

20. Rooney MS, Shukla SA, Wu CJ, et al. Molecular and genetic properties of tumors associated with local immune cytolytic activity. *Cell*. 2015;160:48-61.

21. Subramanian A, Tamayo P, Mootha VK, et al. Gene set enrichment analysis: a knowledge-based approach for interpreting genome-wide expression profiles. *Proc Natl Acad Sci USA*. 2005;102:15545-15550.

22. Cardinali DP, Esquifino AI, Srinivasan V, et al. Melatonin and the immune system in aging. *NeuroImmunoModulation*. 2008;15:272-278.

23. Nasrabadi NN, Ataee R, Abediankenari S, et al. Expression of MT2 receptor in patients with gastric adenocarcinoma and its relationship with clinicopathological features. *J Gastrointest Cancer*. 2014;45:54-60.

24. Calvo JR, Gonzalez-Yanes C, Maldonado MD. The role of melatonin in the cells of the innate immunity: a review. *J Pineal Res*. 2013;55:103-120.

25. Miller SC, Pandi-Perumal SR, Esquifino AI, et al. The role of melatonin in immuno-enhancement: potential application in cancer. *Int J Exp Pathol*. 2006;87:81-87.

26. Poplawski T, Chojnacki C, Czubatka A, et al. Helicobacter pylori infection and antioxidants can modulate the genotoxic effects of heterocyclic amines in gastric mucosa cells. *Mol Biol Rep*. 2013;40:5205-5212.

27. Erdemli HK, Akyol S, Armutcu F, et al. Melatonin and caffeic acid phenethyl ester in the regulation of mitochondrial function and apoptosis: The basis for future medical approaches. *Life Sci*. 2016;148:305-312.

28. Mendivil-Perez M, Soto-Mercado V, Guerra-Librero A, et al. Melatonin enhances neural stem cell differentiation and engraftment by increasing mitochondrial function. *J Pineal Res*. 2017;63:e12415.

29. Wu SM, Lin WY, Shen CC, et al. Melatonin set out to ER stress signaling thwarts epithelial mesenchymal transition and peritoneal dissemination via calpain-mediated C/EBPbeta and NFkappaB cleavage. *J Pineal Res*. 2016;60:142-154.

30. Hong Y, Won J, Lee Y, et al. Melatonin treatment induces interplay of apoptosis, autophagy, and senescence in human colorectal cancer cells. *J Pineal Res*. 2014;56:264-274.

31. Chang I, Mitsui Y, Kim SK, et al. Cytochrome P450 1B1 inhibition suppresses tumorigenicity of prostate cancer via caspase-1 activation. *Oncotarget*. 2017;8:39087-39100.

32. Mitsui Y, Chang I, Fukuhara S, et al. CYP1B1 promotes tumorigenesis via altered expression of CDC20 and DAPK1 genes in renal cell carcinoma. *BMC Cancer*. 2015;15:942.

33. Lissoni P, Chilelli M, Villa S, et al. Five years survival in metastatic non-small cell lung cancer patients treated with chemotherapy alone or chemotherapy and melatonin: a randomized trial. *J Pineal Res*. 2003;35:12-15.

34. Wang YM, Jin BZ, Ai F, et al. The efficacy and safety of melatonin in concurrent chemotherapy or radiotherapy for solid tumors: a meta-analysis of randomized controlled trials. *Cancer Chemother Pharmacol*. 2012;69:1213-1220.

35. Lissoni P, Meregalli S, Nosetto L, et al. Increased survival time in brain glioblastomas by a radioneuroendocrine strategy with

radiotherapy plus melatonin compared to radiotherapy alone. *Oncology*. 1996;53:43-46.

36. Cerea G, Vaghi M, Ardizzoia A, et al. Biomodulation of cancer chemotherapy for metastatic colorectal cancer: a randomized study of weekly low-dose irinotecan alone versus irinotecan plus the oncostatic pineal hormone melatonin in metastatic colorectal cancer patients progressing on 5-fluorouracil-containing combinations. *Anticancer Res*. 2003;23:1951-1954.

37. Lissoni P, Paolorossi F, Ardizzoia A, et al. A randomized study of chemotherapy with cisplatin plus etoposide versus chemoendocrine therapy with cisplatin, etoposide and the pineal hormone melatonin as a first-line treatment of advanced non-small cell lung cancer patients in a poor clinical state. *J Pineal Res*. 1997;23:15-19.

38. Saini N, Gordenin DA. Somatic mutation load and spectra: a record of DNA damage and repair in healthy human cells. *Environ Mol Mutagen*. 2018;59:672-686.

39. Castle JC, Kreiter S, Diekmann J, et al. Exploiting the mutanome for tumor vaccination. *Cancer Res*. 2012;72:1081-1091.

40. Majidinia M, Sadeghpour A, Mehrzadi S, et al. Melatonin: a pleiotropic molecule that modulates DNA damage response and repair pathways. *J Pineal Res*. 2017;63:e12416.

41. Maestroni GJ. The immunoneuroendocrine role of melatonin. *J Pineal Res*. 1993;14:1-10.

42. Maestroni GJ. Therapeutic potential of melatonin in immunodeficiency states, viral diseases, and cancer. *Adv Exp Med Biol*. 1999;467:217-226.

43. Espino J, Rodriguez AB, Pariente JA. The inhibition of TNF-alpha-induced leucocyte apoptosis by melatonin involves membrane receptor MT1/MT2 interaction. *J Pineal Res*. 2013;54:442-452.

SUPPORTING INFORMATION

Additional supporting information may be found online in the Supporting Information section at the end of the article.

How to cite this article: Lv J-W, Zheng Z-Q, Wang Z-X, et al. Pan-cancer genomic analyses reveal prognostic and immunogenic features of the tumor melatonergic microenvironment across 14 solid cancer types. *J Pineal Res*. 2019;66:e12557. https://doi.org/10.1111/jpi.12557